Supporting Information

Le et al. 10.1073/pnas.0915020107

Text S1: Evidence That Excludes the Involvement of Ca^{2+} in the Blocking Effect of COX-2 on LTD Induction

Depolarization-Induced Ca^{2+} Spikes. We applied depolarizing currents of 0.8–1.2 nA (duration, 1 s) to a PC. Induction of fast Na^{+} spikes normally seen (Fig. S2*A*) was blocked by tetrodotoxin (TTX) perfusion (Fig. S2*B*). After recording the remaining slow Ca^{2+} spikes for 5 min, a COX-2 inhibitor was added to the perfusates for another 5 min (Fig. S2*C*). As an index of Ca^{2+} spike excitability, we counted the number of slow Ca^{2+} spikes evoked by each depolarizing rectangular current, and compared the average number between the two phases of perfusion with and without a COX-2 inhibitor (Fig. S2*D*). COX-2 inhibitors did not affect the average number so obtained (Fig. S2*E*). Ca^{2+} spike ratio tends to decrease slightly to less than 100% under perfusion of not only COX-2 inhibitors but also TTX alone. This might be due to a nonspecific decrease in Ca^{2+} spike excitability during prolonged recording.

CF-Evoked Complex Spikes. Complex spikes were evoked in a PC by stimulating CFs in the white matter or granule cell layer (Fig. S2*F*). A comparison between the first 10 min under normal perfusates (Fig. S2*G*) and another 10 min under 0.5 μM DuP 697 (Fig. S2*H* reveals that the COX-2 inhibitor exerted no appreciable effect on the rising slope of the first spike of the complex spikes, which reflects Ca^{2+} influx (1). The rate-of-rise ratio tended to slightly decrease, but was not specific to COX-2 inhibitors (Fig. S2*I*) and may have been due to rundown of Ca^{2+} fluxes in CF-evoked complex spikes during prolonged recording.

Ca^{2+} Imaging. Purkinje cells were visualized through a ×60 immersion objective using infrared differential interference contrast optics. The patch pipette (3–4 MΩ) containing a Ca^{2+} indicator, 200 μM Oregon Green 488 BAPTA-1 (Molecular Probes), was attached to a Purkinje cell soma. Measurements were started 20 min after the formation of whole-cell patch configuration to allow sufficient infusion of the Ca^{2+} indicator. Parallel fibers (PFs) were stimulated using a glass electrode (tip diameter, 5–8 μm) placed in the molecular layer. The dendritic region of the Purkinje cell receiving synapses from the stimulated PFs was located by observing an increase in the intensity of fluorescent signals generated by PF stimulation with 10 pulses at 100 Hz. Images were captured at a frame rate of 35 ms for 10 s using a confocal laser scanning microscope (FLUOVIEW FV1000, Olympus). Conjunctive stimulation (Cj) was performed in combination of 2 PF stimuli at 30 ms intervals and somatic depolarization from −70 to −20 mV for 150 ms, repeated at 1 Hz for 5 min. Fluorescence intensity was recorded before, during, and after conjunctive stimulation. Changes in fluorescence intensity were normalized relative to the average intensity recorded before conjunctive stimulation. COX-2 inhibitors were bath-applied for 15 min from 5 min before Cj (details in Fig. S3).

Text S2: Additional Data on LTD

In this study, we tested LTD by means of gene knockout of $cPLA_2\alpha$ and numerous pharmacological reagents in various combinations. To save space in printed pages, substantial parts of them are illustrated here. Figs. S1 and S4 are formulated similarly to Fig. 2 and Fig. 3, and are cited in the text as supportive evidence. Another set of supplementary data about drugs used (Table S1) and LTD magnitudes (Table S2) are also included in *SI Text.*

A comment is made here regarding Fig. S1*B,* in which LTD is blocked by pyrrolidine-1 at 0.4 μM but not at 0.3 μM. This contrasting dose–effect relationship in Fig. S1*B (Inset)* can be explained based on the observation (2) that AA release from CHO cells occurs at an IC_{50} in the 0.2–0.5 μM range. The amount of AA released can be substantial at 0.3 μM or lower concentrations of pyrrolidine-1, but it decreases sharply at 0.4 μM or higher concentrations. Therefore, LTD may not be affected by pyrrolidine-1 at 0.2–0.3 μM, but may be abolished at 0.4–0.5 μM.

Text S3: Details of Method of OKR Measurement

OKR was measured with the method previously used (3, 4). Under isoflurane (Escain, Mylan-Japan) anesthesia and aseptic conditions, a platform for head fixation was constructed on the cranial bone using one bolt (15 mm long and 2 mm across) and synthetic resin. More than 2 days after surgery, a mouse was mounted in a plastic holder set in the center of a cylindrical checked-pattern screen (screen diameter and height, 60 cm), with the head fixed and the body loosely constrained. Eye movements were recorded using an infrared television camera for real-time recording. OKR was examined by 15° sinusoidal screen oscillation at 0.17 Hz (maximum screen velocity, 7.9°/s) in light. More than 10 cycles of the evoked eye movements free of blinks and saccades were averaged, and a modified Fourier analysis was carried out to determine the mean amplitude and phase. The gain of eye movements was defined as the ratio of the peak-to-peak amplitude of eye movements to that of the screen oscillation. OKR adaptation was examined by exposing the mouse to 1 h of sustained 15°, 0.17-Hz sinusoidal screen oscillation in light.

1. Rokni D, Yarom Y (2009) State-dependence of climbing fiber-driven calcium transients in Purkinje cells. *Neuroscience* 162:694–701.
2. Ghomashchi F, et al. (2001) A pyrrolidine-based specific inhibitor of cytosolic phospholipase $A_2\alpha$ blocks arachidonic acid release in a variety of mammalian cells. *Biochim Biophys Acta Biomembranes* 1513:160–166.
3. Katoh A, Kitazawa H, Itohara S, Nagao S (2000) Inhibition of nitric oxide synthesis and gene knockout of neuronal nitric oxide synthase impaired adaptation of mouse optokinetic response eye movements. *Learn Mem* 7:220–226.
4. Shutoh F, Ohki M, Kitazawa H, Itohara S, Nagao S (2006) Memory trace of motor learning shifts transsynaptically from cerebellar cortex to nuclei for consolidation. *Neuroscience* 139:767–777.

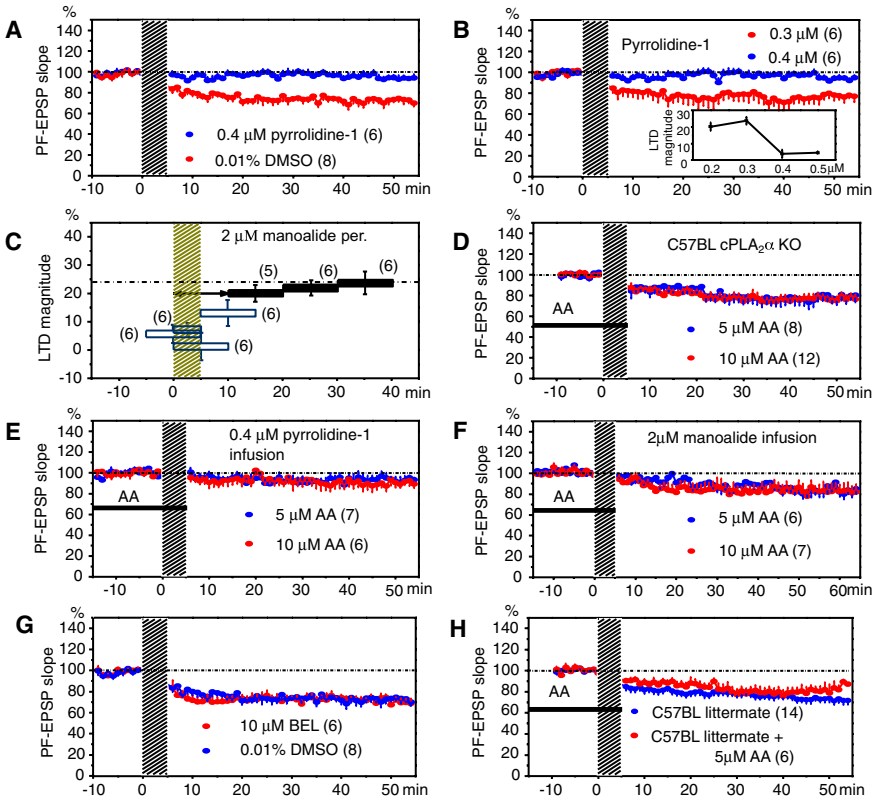

Fig. S1. Supplementary data on the involvement of PLA_2 and arachidonic acid (AA) in LTD. *(A)* LTD blockade by pyrrolidine-1 as contrasted to the control plots obtained with the infusion of DMSO alone. (*B*) Dose-dependence of pyrrolidine-1 effect. (*C*) LTD magnitude–perfusion time relationship for manoalide. Horizontal broken line indicates LTD magnitude determined for 0.01% DMSO perfusion for 20 min overlapping conjunction (24.3%). Error bars represent SD. (*D*) AA perfusion for 20-min before and during conjunction rescued the LTD blocked in null deficiency of $cPLA_2\alpha$. AA at 5 and 10 μM restored LTD equally effectively, suggesting that 5 μM AA maximally causes LTD. (*E*) AA only weakly restored the LTD blocked by pyrrolidine-1. (*F*) A substantially rescued the LTD blocked by 2 μM manoalide. (*G*) Minimal effects of infusion of $iPLA_2$-specific inhibitor, bromoenol lactone (BEL), on LTD as compared with DMSO infusion. (*H*) When LTD was induced normally in C57BL littermate, perfusion of 5 μM AA attenuated LTD slightly.

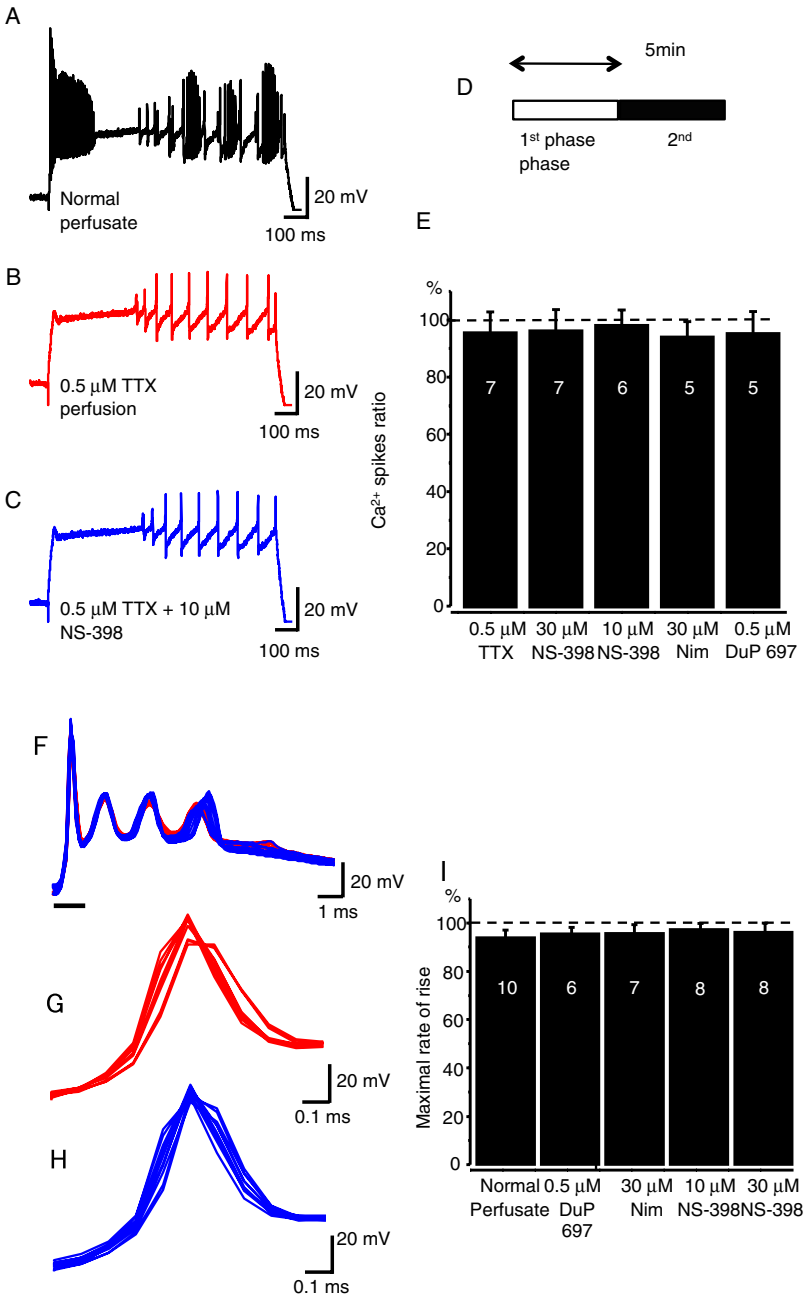

Fig. S2. Effect of COX-2 inhibitors on Ca^{2+} spikes and complex spikes in PCs. (*A–C*) Specimen records taken from the same PC under different perfusates as indicated. (*D*) Perfusion scheme with sequential two phases, each lasting 5 min. TTX was perfused throughout both phases, whereas in the second phase, a COX-2 inhibitor was added except for the control. (*E*) Column size, ratio of the average number of Ca^{2+} spikes counted during the second phase relative to that during the first phase. Error bars in *E* and *I* represent SD. Numbers in columns are those of Purkinje cells tested. Under columns, the inhibitors added in the second phase are indicated. Nim, nimesulide. (*F*) Complex spikes evoked in a PC by 0.2 Hz CF stimulation for 10 min. Records taken in the first phase (red) for 10 min under normal perfusates and second phase (blue) for another 10 min under 0.5 μM DuP 697 are superimposed, closely overlapping each other. (*G*, *H*) The first spike of the complex spikes (indicated by a horizontal bar) shown in an expanded time scale. Ten traces, each representing the average for 1 min, are superimposed. (*I*) Maximum rates of rise for the first spikes averaged for 10 min in the presence of the perfusates indicated, relative to those averaged under normal perfusates during the preceding 10 min.

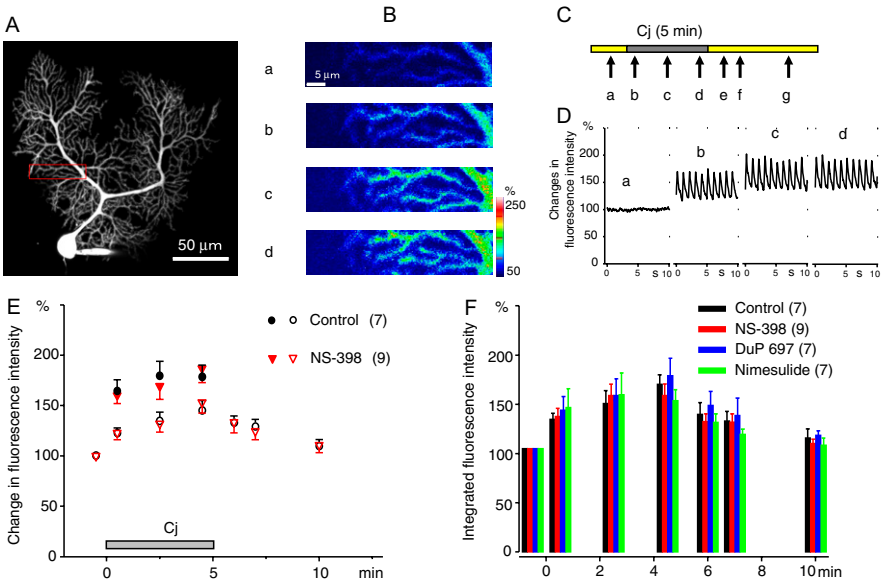

Fig. S3. Effects of COX-2 inhibitors tested by Ca^{2+} imaging in PCs. (*A*) Purkinje cell profile. Red line encloses dendritic input region, within which 10 PF stimuli at 100 Hz evoked Ca^{2+} signals. (*B*) Ca^{2+} signals evoked by Cj in dendritic input region in *A* taken at different times (*a*–*d*) shown in *C*. (*C*) Experimental scheme. Upward arrows (*a*– *g*) indicate timing of recording dendritic Ca^{2+} signals: a, –0.5 min before onset; b, c, and d, 0.5, 2.5, and 4.5 min after onset; and e, f, and g, 1, 2, and 5 min after cessation of Cj. (*D*) Specimen curves showing changes in fluorescence intensity as recorded from a spot chosen in the dendritic input region of the same PC during 10-s imaging times at *a*–*d* as indicated in *C*. For curves at *b*– *d*, note the sharp increase to a peak and decrease to the baseline of fluorescence intensity following each application of Cj stimulus. Note also that the baseline shifts upward during repeated Cj. (*E*) Changes in fluorescence intensity observed during the last 3 s of the 10-s imaging time. Filled symbols indicate peak fluorescence intensity relative to the fluorescence intensity observed before conjunction (*a*). Hollow symbols indicate the baseline fluorescence intensity. Gray bar indicates Cj. (*F*) Fluorescence intensity time-integrated for 3 s In *E* and *F*, color codes as indicated. Error bars in *E* and *F*, SEM. Two-way ANOVA showed that none of the perfused three types COX-2 inhibitors significantly affected the fluorescence intensity associated with Cj; $P = 0.76$ for baseline values and $P = 0.46$ for peak values in *E*, and $P = 0.63$ for integated fluorescence in *F*.

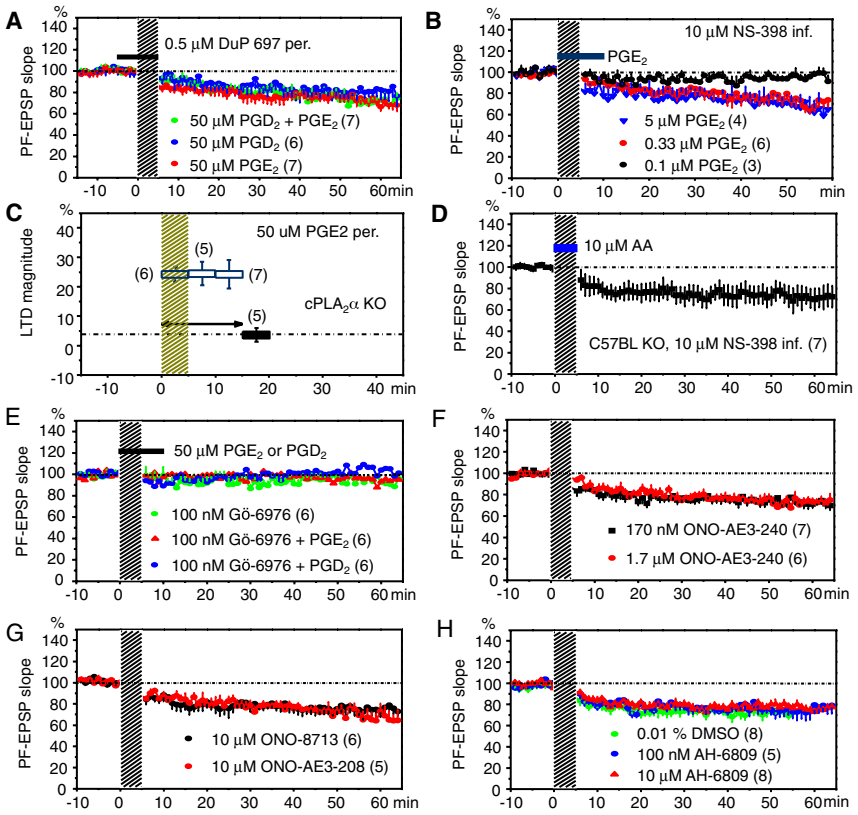

Fig. S4. Effects of COX-2 inhibitors and PGD_2/E_2 on LTD. *(A)* Rescue of DuP 697-perfusion-induced LTD blockade by the infusion of PGD_2/E_2. *(B)* Rescue of NS-398-infusion–induced LTD blockade by perfusion of PGE_2 at low concentrations. *(C)* Mapping the window for rescuing LTD by perfusion of 50 μM PGE_2 in $cPLA_2\alpha$ KO Purkinje cells. Error bars, SD. *(D)* Five-min perfusion of AA also rescues LTD blocked by the combination of $cPLA_2\alpha$ KO and COX-2 inhibition. (*E*) Ten-minute perfusion of PGD_2/E_2 has no effect on LTD blocked by continuous infusion of 100 nM Gö 6976, specific PKC inhibitor. (*F*) Minimal effects of EP3 antagonist on LTD at two concentrations. (*G*) Minimal effects of EP1 and EP4 antagonists. (*H*) Minimal effects of AH 6809, nonspecific prostanoid receptor antagonist at two concentrations, compared with that of 0.01% DMSO used as solvent (Table S1).

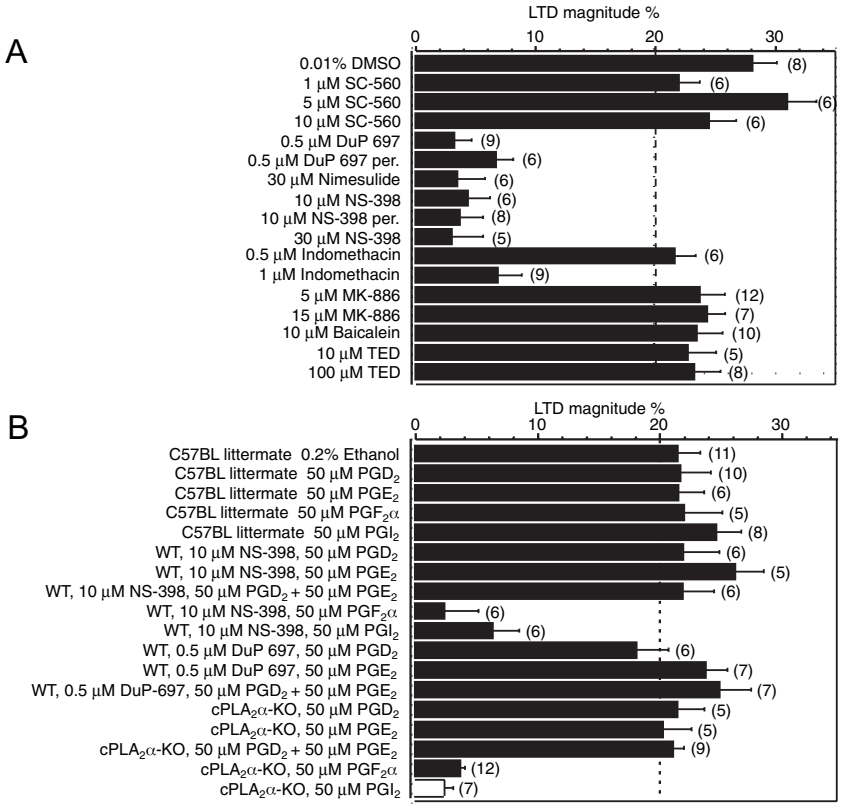

Fig. S5. Comparison of LTD magnitudes. (*A*) For COX-2 inhibitors. Error bars represent SD. Numbers in parentheses are numbers of Purkinje cells tested. (*B*) For prostaglandins. Illustrated similarly to *A*. One open column represents the negative value of LTD magnitude.

Table S1. Pharmacological reagents used for testing LTD

Reagent	Source	Effect	IC_{50} (nM)	Conc. (μM)	Solvent	Applied by	Ref.
AA-Na	Tocris	Exogenous AA		5, 10, or 20	Water	per.	
AH 6809	Tocris	EP1/2, DPAntagonist	500 for EP1 5000 for EP2/DP	0.1, 0.2 or 10	DMSO	inf.	1
Baicalein	BIOMOL	12-LO inhibitor	120 (platelet)9.5 (Macrophage)	10	DMSO	inf.	2
BEL	Cayman	$iPLA_2$ inhibitor	60	10	DMSO	inf.	3
DuP 697	Tocris	COX-2 inhibitor	10	0.5	DMSO	inf./per.	4
Gö 6976	BIOMOL	PKC inhibitor	2.3 (α), 6.2 (β), 20 (γ)	0.1	DMSO	inf.	5
Indomethacin	Tocris	COX-1/2 inhibitor	230/630	0.5, 1 or 5	Ethanol	inf.	6
Manoalide	Wako	$cPLA_2\alpha$ inhibitor		1 or 2	DMSO	inf./per.	7
MK-886	BIOMOL	5-LO inhibitor	2.5	5 or 15	DMSO	inf.	8
Nimesulide	Sigma	COX-2 inhibitor		30	DMSO	inf.	4
ONO-8713	ONO Pharm	EP1 antagonist	920	10	DMSO	inf.	9
ONO-AE3-240	ONO Pharm	EP3 antagonist	17	0.17 or 1.7	DMSO	inf.	10
ONO-AE3-208	ONO Pharm	EP4 antagonist		10	DMSO	inf.	9
NS-398	Tocris	COX-2 inhibitor	3800	10 or 30	DMSO	inf./per.	4
PGD_2	Sigma	Prostaglandin D_2		50 or 0.33	Ethanol	inf./per.	11
PGE_2	Sigma	Prostaglandin E_2		0.1, 0.33, 1, 50	Ethanol	inf./per.	11
$PGF_{2\alpha}$	Sigma	Prostaglandin $F_{2\alpha}$		50	Ethanol	inf.	11
PGI_2 –Na	Tocris	Prostaglandin I_2		50	Ethanol	inf.	11
Picrotoxin	Sigma	$GABA_A$ antagonist		100	ACSF	per.	
Pyrrolidine-1	Calbiochem	$cPLA_2\alpha$ inhibitor	1.8	0.1, 0.2, 0.3, 0.4, or 0.5	DMSO	inf./per.	1213
SC 560	Sigma	COX-1 inhibitor	9	1, 5, or 10	DMSO	per.	14
SC 19220	Sigma	EP1 antagonist	6700	10	DMSO	inf.	15
SC-51089	BIOMOL	EP1 antagonist	15000	10	DMSO	inf.	16
SC-51322	BIOMOL	EP1 antagonist		10	DMSO	inf.	17
TED	Sigma	5-LO inhibitor12-LO inhibitor15-LO inhibitor	90 13 500	10 or 100	DMSO	inf.	18
TPA	Calbiochem	PKC activator		0.5	DMSO	per.	1920

AA, arachidonic acid; BEL, bromoenol lactone; Na-, sodium salt; TED, (1-thienyl)ethyl 3,4-dihydroxy-benzylidene-cyanoacetate; TPA, 2-O-tetradecanoyl phorbol-13-acetate. DMSO and ethanol were used at 0.01 and 0.2%, respectively. inf., infusion; per., perfusion; ONO Pharm, ONO Pharmaceutical Co., Ltd.

1. Xie G, et al. (2003) 5-Hydroxytryptamine-induced plasma extravasation in the rat knee joint is mediated by multiple prostaglandins. *Inflamm Res* 52:32–38.
2. Deschamps JD, Kenyon VA, Holman TR (2006) Baicalein is a potent in vitro inhibitor against both reticulocyte 15-human and platelet 12-human lipoxygenases. *Bioorgan Med Chem* 14: 4295–4301.
3. St-Gelais F, et al. (2004) Postsynaptic injection of calcium-independent phospholipase A_2 inhibitors selectively increases AMPA receptor-mediated synaptic transmission. *Hippocampus* 14:319–325.
4. Flower RJ (2003) The development of COX-2 inhibitors. *Nat Rev Drug Discovery* 2:179–191.
5. Jideama NM, et al. (1993) Phosphorylation specificities of protein kinase c isozymes for bovine cardiac troponin i and troponin t and sites within these proteins and regulation of myofilament properties. *J Biol Chem* 268:9194–9197.
6. Palomer A, et al. (2002) Identification of novel cyclooxygenase-2 selective inhibitors using pharmacophore models. *J Med Chem* 45:1402–1411.
7. Linden D (1995) Phospholipase A_2controls the induction of short-term versus long-term depression in the cerebellar Purkinje neuron in culture. *Neuron* 15:1393–1401.
8. Mancini JA, et al. (1992) 5-Lipoxygenase-activating protein is the target of a novel hybrid of two classes of leukotriene biosynthesis inhibitors. *Mol Pharmacol* 41:267–272.
9. Ohnishi A, et al. (2001) EP1 and EP4 receptors mediate exocytosis evoked by prostaglandin E_2 in guinea-pig antral mucous cells. *Exp Physiol* 86:451–460.
10. Amano H, et al. (2003) Host prostaglandin E_2-EP3 signaling regulates tumor-associated angiogenesis and tumor growth. *J Exp Med* 197:221–232.
11. Akaneya Y, Tsumoto T (2006) Bidirectional trafficking of prostaglandin E_2 receptors involved in long-term potentiation in visual cortex. *J Neurosci* 26:10209–10221.
12. Seno K, et al. (2000) Pyrrolidine inhibitors of human cytosolic phospholipase A_2. *J Med Chem* 43:1041–1044.
13. Ghomashchi F, Stewart A, Hefner Y, Ramanadham S, Turk J, Leslie CC, Gelb MH (2001) A pyrrolidine-based specific inhibitor of cytosolic phospholipase $A_2\alpha$ blocks arachidonic acid release in a variety of mammalian cells. *Biochim. Biophys. Acta Biomembranes* 1513:160–166.
14. Smith CJ, et al. (1998) Pharmacological analysis of cyclooxygenase-1 in inflammation. *Proc Natl Acad Sci USA* 95:13313–13318.
15. Kiriyama M, et al. (1997) Ligand binding specificities of the eight types and subtypes of the mouse prostanoid receptors expressed in Chinese hamster ovary cells. *Br J Pharmacol* 122: 217–224.
16. Matlhagela K, Taub M. (2006) Involvement of EP1 and EP2 receptors in the regulation of the Na, K-ATPase by prostaglandins in MDCK cells. *Prostagland Other Lipid Mediat* 79:101–113.
17. Kanamori Y, et al. (1997) Migration of neutrophils from blood to tissue: Alteration of modulatory effects of prostanoid on superoxide generation in rabbits and humans. *Life Sci* 60: 1407–1417.
18. Cho H, et al. (1991) Novel caffeic acid derivatives: Extremely potent inhibitors of 12-lipoxygenase. *J Med Chem* 34:1503–1505.
19. Endo S, Launey T. (2003) ERKs regulate PKC-dependent synaptic depression and declustering of glutamate receptors in cerebellar Purkinje cells. *Neuropharmacology* 45:863–872.
20. Tanaka K, Augustine GJ (2008) A positive feedback signal transduction loop determines timing of cerebellar long-term depression. *Neuron* 59:608–620.

Table S2. LTD magnitude under various conditions

No.	Stimuli	Figure	Mouse types	Drugs applied	LTD Magnitude	Blocked LTD
1	Cj (=2PF+md)	2*A*	C3H WT		26.3% ± 3.8% (5)	
2	Cj	2*A*	C57BL WT		29.2% ± 1.4% (9)	
3	2PF+CF		C57BL WT		27.0% ± 3.2% (7)	
4	Cj		C57BL WT	Low K^+ concentration (solution B).	24.5% ± 2.5% (6)	
5	2PF	2*A*	C57BL WT			3.0% ± 1.9% (10)
6	Md	2*A*	C57BL WT			3.2% ± 2.4% (11)
7	Cj	2*B*	C3H cPLA$_2\alpha$ KO			2.9% ± 2.3% (13)
8	2PF+CF		C3H cPLA$_2\alpha$ KO			3.0% ± 2.2% (7)
9	Cj	2*B*	C57BL cPLA$_2\alpha$ KO			3.9% ± 0.6% (31)
11	Cj	2*B*	C3H littermate		25.7% ± 1.1% (10)	
12	2PF+CF		C3H littermate		24.2% ± 1.5% (9)	
13	Cj	2*B*	C57BL littermate		26.3% ± 1.3% (14)	
14	Cj	2*C*, S4*A* and *B*	C57BL WT	0.4 μM pyrrolidine-1 inf.		4.7% ± 1.8% (6)
15	Cj	S3*G*	C57BL WT	0.01% DMSO inf.	27.8% ± 2.0% (8)	
16	Cj	S3*G*	C57BL WT	10 μM BEL inf.	28.0% ± 2.3% (6)	
17	Cj	2*E*	C57BL cPLA$_2\alpha$ KO	5 μM AA per.	22.4% ± 2.5% (8)	
18	Cj	S3*D*	C57BL cPLA$_2\alpha$ KO	10 μM AA per.	23.5% ± 1.2% (12)	
19	Cj		C3H cPLA$_2\alpha$ KO	10 μM AA per.	23.0% ± 1.7% (11)	
20	Cj	S3*E*	C57BL WT	0.4 μM pyrrolidine-1 inf. + 10 μM AA per.	10.0% ± 2.1% (6)	
21	Cj	S3*F*	C57BL WT	2 μM manoalide inf. + 10 μM AA per.	16.1% ± 2.1% (7).	
22	Cj	S3H	C57BL littermate	5 μM AA per.	20.1% ± 1.0.3% (6)	
23	Cj		C3H littermate	10 μM AA per.	15.2% ± 2.2% (6)	
24	NS		C57BL WT	5 μM AA, 20-min per.		6.9% ± 2.5% (3)
25	Cj	S5*A*	C57BL WT	0.5 μM DuP 697 inf.		2.9% ± 1.4% (9)
26	Cj	S5*A*	C57BL WT	30 μM Nimesulide inf.		3.2% ± 2.3% (6)
27	Cj	S5*A*	C57BL WT	10 μM NS-398 inf.		4.5% ± 1.4% (6)
28	Cj	S5*A*	C57BL WT	30 μM NS-398 inf.		2.7% ± 2.6% (5)
29	Cj	S5*A*	C57BL WT	1.0 μM Indomethacin inf.		6.6% ± 2.0% (9)
30	Cj	S5*A*	C57BL WT	0.5 μM Indomethacin inf.	21.3% ± 1.8% (6)	
31	Cj	S5*A*	C57BL WT	1 μM SC-560 (COX-1 inhibitor) inf.	21.7% ± 1.7% (6)	
32	Cj	S5*A*	C57BL WT	5 μM SC-560 (COX-1 inhibitor) inf.	30.7% ± 2.4% (6)	
33	Cj	S5*A*	C57BL WT	10 μM SC-560 (COX-1 inhibitor) inf.	24.2% ± 2.3% (6)	
34	Cj	S5*A*	C57BL WT	5 μM MK-886 inhibiting 5-LO inf.	23.4% ± 2.1% (12)	
35	Cj	S5*A*	C57BL WT	15 μM MK-886 inhibiting 5-LO inf.	24.0% ± 1.5% (7)	
36	Cj	S5*A*	C57BL WT	10 μM Baicalein inhibiting 12-LO inf.	23.1% ± 2.2% (10)	
37	Cj	S5*A*	C57BL WT	10 μM TED inhibiting 5-, 12-, or 15-LO inf.	22.4% ± 2.3% (5)	
38	Cj	S5*A*	C57BL WT	100 μM TED inhibiting 5-, 12-, or 15-LO inf.	22.9% ± 2.2% (8)	
39	Cj	3*A*	C57BL WT	10 μM NS-398 per.		3.4% ± 2.0% (8)
40	Cj	S5*B*	C57BL WT	10 μM NS-398 per. + 50 μM PGD_2 inf.	21.6% ± 2.9% (6)	
41	Cj	S5*B*	C57BL WT	10 μM NS-398 per. + 50 μM PGE_2 inf.	25.9% ± 2.3% (5)	
42	Cj	S5*B*	C57BL WT	10 μM NS-398 per. + 50 μM PGD_2 + PGE_2 inf.	21.6% ± 2.6% (6)	
43	Cj	S5*B*	C57BL WT	10 μM NS-398 per. + 50 μM $PGF_{2\alpha}$ inf.		2.1% ± 2.8% (6)
44	Cj	S5*B*	C57BL WT	10 μM NS-398 per. + 50 μM PGI_2 inf.		6.0% ± 2.2% (6)
45	Cj	S5*B*	C57BL WT	0.5 μM DuP 697 per.		6.4% ± 1.5% (6)
56	Cj	S4*A*	C57BL WT	0.5 μM DuP 697 per.+ 50 μM PGD_2 inf.	17.8% ± 2.6% (6)	
47	Cj	S4*A*	C57BL WT	0.5 μM DuP 697 per.+ 50 μM PGE_2 inf.	23.5% ± 1.8% (7)	
48	Cj	S4*A*	C57BL WT	0.5 μM DuP 697 per.+ 50 μM PGD_2 + PGE_2 inf.	24.6% ± 2.6% (7)	
49	Cj	S4*B*	C57BL WT	10 μM NS-398 inf. + 5 μM PGE_2 10 min per.	28.5% ± 2.3 (4)	

Table S2. Cont.

No.	Stimuli	Figure	Mouse types	Drugs applied	LTD Magnitude	Blocked LTD
50	Cj	S4*B*	C57BL WT	10 μM NS-398 inf. + 0.33 μM PGE_2 10 min per.	22.5% ± 2.2% (6)	
51	Cj	S4*B*	C57BL WT	10 μM NS-398 inf. + 0.1 μM PGE_2 10 min per.		5.1% ± 1.6 (3)
52	Cj		C57BL WT	10 μM NS-398 inf. + 5 μM PGD_2 10 min per.	21.0% ± 1.6% (3)	
53	Cj		C57BL WT	10 μM NS-398 inf. + 0.33 μM PGD_2 10 min per.	22.8% ± 2.2% (4)	
54	Cj	S5*B*	C57BL littermate	50 μM PGD_2 inf.	21.4% ± 2.5% (10)	
55	Cj	S5*B*	C57BL littermate	50 μM PGE_2 inf.	21.2% ± 2.2% (6)	
56	Cj	S5*B*	C57BL littermate	50 μM PGD_2 + 50 μM PGE_2 inf.	21.3% ± 2.8% (5)	
57	Cj	S5*B*	C57BL littermate	50 μM $PGF_2\alpha$ inf.	21.7% ± 3.1% (5)	
58	Cj	S5*B*	C57BL littermate	50 μM PGI_2 inf.	24.3% ± 2.0% (8)	
59	Cj	S5*B*	C57BL littermate	0.2% ethanol inf.	21.2% ± 1.9% (11)	
60	Cj	S5*B*	C57BL cPLA$_2\alpha$ KO	50 μM PGD_2 inf.	21.1% ± 2.0.2% (5)	
61	Cj	S5*B*	C57BL cPLA$_2\alpha$ KO	50 μM PGE_2 inf.	20.0% ± 2.0.3% (5)	
62	Cj	S5*B*	C57BL cPLA$_2\alpha$ KO	50 μM PGD_2 + 50 μM PGE_2 inf.	20.8% ± 0.0.9% (9)	
63	Cj	S5*B*	C57BL cPLA$_2\alpha$ KO	50 μM PGI_2 inf.		−2.1% ± 2.3% (7)
64	Cj	S5*B*	C57BL cPLA$_2\alpha$ KO	50 μM $PGF_2\alpha$ inf.		3.4% ± 1.1% (12)
65	Cj		C57BL cPLA$_2\alpha$ KO	0.2% ethanol inf.		0.4% ± 2.5% (9)
66	Cj	3*E*	C57BL cPLA$_2\alpha$ KO	50 μM PGE_2 5 min per.	24.2% ± 1.9% (6)	
67	Cj	S4*D*	C57BL cPLA$_2\alpha$ KO	10 μM NS-398 inf. + 10 μM AA 5 min per.	26.2% ± 1.9% (7)	
68	Chem	3*F*	C57BL WT	0.5 μM TPA 15min per.		8.8% ± 1.9 (9)
69	Chem	3*F*	C57BL WT	0.5 μM TPA 15min per. + 50 μM PGE_2 10 min per.	20.9% ± 3.1% (6)	
70	Cj	S4*E*	C57BL WT	100 nM Gö 6976 inf.		4.2% ± 2.3% (6)
71	Cj	S4*E*	C57BL WT	100 nM Gö 6976 inf.+ 50 μM PGD_2 per.		3.5% ± 2.7% (6)
72	Cj	S4*E*	C57BL WT	100 nM Gö 6976 inf.+ 50 μM PGE_2 per.		−1.4% ± 1.3% (6)
73	Cj	S4*G*	C57BL WT	10 μM ONO-8713 inf.	24.7% ± 1.1% (6)	
74	Cj	S4*F*	C57BL WT	170 nM ONO-AE3-240 inf.1.7 μM ONO-AE3-240 inf.	25.2% ± 1.9% (7) 25.3% ± 1.4% (6)	
75	Cj	S4*G*	C57BL WT	10 μM ONO-AE3-208 inf.	26.6% ± 2.3% (5)	
76	Cj		C57BL WT	10 μM SC-19220 inf.	26.9% ± 2.7% (5)	
77	Cj		C57BL WT	10 μM SC-51089 inf.	22.3% ± 1.7% (5)	
78	Cj		C57BL WT	10 μM SC-51322 inf.	24.7% ± 2.3% (7)	
79	Cj	S4*H*	C57BL WT	100 nM AH-6809 inf.	22.0% ± 2.6% (5)	
80	Cj	S4*H*	C57BL WT	10 μM AH-6809 inf.	21.5% ± 2.0% (8)	

Chem, chemical stimulation with TPA; Cj, conjunction of double-shock PF stimulation of PFs (2PF) and membrane depolarizing pulses (md); No., experiment number; NS, no stimulus. For drugs applied, refer to Table S1. LTD magnitude represents the average decrease in PF-EPSP slopes at 41–50 min relative to the 5-min preconjunction period, and is indicated as mean ± SEM % (number of cells tested). Blocked LTD, measured similarly to LTD magnitudes but during blockade of LTD. Data were obtained in solution A except for case No. 4, obtained in solution B (solutions given in *Materials and Methods*, *In Vitro Cerebellar Slices*).